

Annual Review of Earth and Planetary Sciences
**What Models Tell Us About the
 Evolution of Carbon Sources
 and Sinks over the Phanerozoic**

Y. Godd ris,¹ Y. Donnadieu,² and B.J.W. Mills³

¹G osciences Environnement Toulouse, CNRS–Universit  de Toulouse III, Toulouse, France; email: yves.godderis@get.omp.eu

²Centre Europ en de Recherche et d'Enseignement des G osciences de l'Environnement, CNRS–Aix Marseille Universit , Aix-en-Provence, France

³School of Earth and Environment, University of Leeds, Leeds, United Kingdom

Annu. Rev. Earth Planet. Sci. 2023. 51:471–92

First published as a Review in Advance on
 February 15, 2023

The *Annual Review of Earth and Planetary Sciences* is
 online at earth.annualreviews.org

<https://doi.org/10.1146/annurev-earth-032320-092701>

Copyright   2023 by the author(s). This work is licensed under a Creative Commons Attribution 4.0 International License, which permits unrestricted use, distribution, and reproduction in any medium, provided the original author and source are credited. See credit lines of images or other third-party material in this article for license information.

Keywords

carbon cycle, climate, deep time, weathering, modeling

Abstract

The current rapid increase in atmospheric CO₂, linked to the massive use of fossil fuels, will have major consequences for our climate and for living organisms. To understand what is happening today, it is informative to look at the past. The evolution of the carbon cycle, coupled with that of the past climate system and the other coupled elemental cycles, is explored in the field, in the laboratory, and with the help of numerical modeling. The objective of numerical modeling is to be able to provide a quantification of the processes at work on our planet. Of course, we must remain aware that a numerical model, however complex, will never include all the relevant processes, impacts, and consequences because nature is complex and not all the processes are known. This makes models uncertain. We are still at the beginning of the exploration of the deep-time Earth. In the present contribution, we review some crucial events in coupled Earth-climate-biosphere evolution over the past 540 million years, focusing on the models that have been developed and what their results suggest. For most of these events, the causes are complex and we are not able to conclusively pinpoint all causal relationships and feedbacks in the Earth system. This remains a largely open scientific field.

- The era of the pioneers of geological carbon cycle modeling is coming to an end with the recent development of numerical models simulating the physics of the processes, including climate and the role of vegetation, while taking into account spatialization.

ANNUAL
REVIEWS **CONNECT**

www.annualreviews.org

- Download figures
- Navigate cited references
- Keyword search
- Explore related articles
- Share via email or social media



- Numerical models now allow us to address increasingly complex processes, which suggests the possibility of simulating the complete carbon balance of objects as complex as a mountain range.
- While most of the processes simulated by models are physical-chemical processes in which the role of living organisms is taken into account in a very simple way, via a limited number of parameters, models of the carbon cycle in deep time coupled with increasingly complex ecological models are emerging and are profoundly modifying our understanding of the evolution of our planet's surface.

1. INTRODUCTION

The ongoing rise in atmospheric CO₂, sustained by the massive release of fossil carbon by human activities, is the cause of ongoing and future climate change (IPCC 2021). Understanding the link between the carbon release and the CO₂ concentration in the atmosphere requires an accurate description of the global carbon cycle, and of other coupled elemental cycles, such as those of oxygen, calcium, and nutrients such as phosphorus, nitrogen, and iron. One of the main challenges for the scientific community is the prediction of the future evolution of Earth's climate and of the carbon cycle. As there are no data for the future, past climates have been explored to validate methods of prediction of the future climate (Tierney et al. 2020). Most efforts have been concentrated on Quaternary climate (between the present and 2.58 million years ago, Ma), with the setup of international intercomparison programs such as the PMIP (Paleoclimate Modelling Intercomparison Project) initiative (Braconnot et al. 2007).

There is also value in going further back in time, exploring pre-Quaternary, or deep-time, climates. Models have been used to reconstruct the climate up to about 800 million years in the past (the Neoproterozoic) and even to explore the climate of the Archean. There are multiple reasons why a few pioneers started to run numerical models in the early 1980s to reconstruct deep-time climate (Barron 1983). One of the arguments often put forward is that the climate of the last million years was generally colder than the current and the future climate. Thus, even though it contained occasional warm interglacial events, the Quaternary might not be the most appropriate time to constrain climate models.

If we are looking for periods characterized by a warmer climate than the present one, we have to look to deep time (Tierney et al. 2020). Sedimentological studies reveal a plethora of deep-time examples of warmer climates, with flat equator-to-pole temperature gradients and without icecaps. The Cenomanian–Turonian period of the Cretaceous, which is considered to be the warmest climatic episode of the Phanerozoic, was among the first deep-time periods for which the climate was numerically simulated (Barron 1983).

When trying to understand the climatic consequences of an increase in CO₂, we cannot limit ourselves to an approach that would consist of imposing a CO₂ level and simulating the corresponding climate because the climate changes caused by an increase in atmospheric CO₂ modify the processes involved in the global carbon cycle. These changes to carbon fluxes can amplify the CO₂ increase and thus act as positive feedbacks. Others can generate negative feedbacks within the carbon cycle, limiting the change in CO₂ concentration. The evolution of climate and that of atmospheric CO₂ must therefore be considered as intimately coupled.

The complex processes that link the climate to the carbon cycle require the implementation of numerical models in order to quantitatively estimate the importance of each of these processes. It is not currently possible to accurately reconstruct the world as it was tens or hundreds of millions

of years ago, so the target for these models is to estimate the sensitivity of the Earth system to the various processes involved in the carbon cycle and in the other coupled elemental cycles.

In this review, we describe the main processes that control the evolution of the carbon cycle and climate on geological timescales (10^5 years or longer). We show how these processes are numerically modeled, emphasizing the contribution of numerical modeling to the understanding of the evolution of Earth's climate, as well as the limitations of current models.

2. TIMESCALES AND RESIDENCE TIMES

We define the surficial Earth system as the coupled atmospheric, oceanic, and biospheric surficial envelopes of Earth. These three envelopes contain about 40,000 gigatons of C (GtC), with the ocean being by far the biggest component (38,000 GtC). Carbon is rapidly cycled through these reservoirs. For instance, an atom of carbon typically stays in the atmosphere for less than 3 years before being transferred to the ocean or to the continental biomass. This mean residence time rises to a few thousands of years for the oceanic reservoir of carbon. In the following discussion, we arbitrarily fix the lower bound of the geological timescale to be 10^5 years.

The surficial Earth system is not a closed system; it is connected to the solid Earth. An atom enters the surficial Earth system following one of two distinct pathways:

1. Release from continental rocks, either through weathering of carbonate rocks or through oxidation of organic carbon-rich sediments outcropping at the surface of the continents. Oxidative weathering of sedimentary organic carbon is estimated to be about 0.08 GtC/year (Lenton et al. 2018), and carbonate weathering at 0.14 GtC/year (Gaillardet et al. 1999).
2. Degassing from the solid Earth, including arc volcanism, metamorphism, and magmatic processes along mid-oceanic ridges. The global degassing flux is estimated at 0.07 ± 0.04 GtC/year (Gerlach 2011).

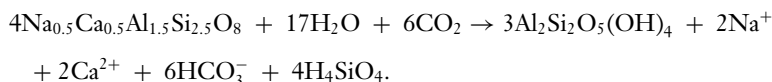
Carbon is then removed by two processes:

1. Carbonate deposition on the seafloor (including sedimentary carbonates and production of carbonate minerals by the weathering of the oceanic crust). Global sedimentary carbonate deposition is estimated to be close to 0.24 GtC/year. The consumption by seafloor weathering is more poorly constrained, estimated at a maximum value of 0.03 GtC/year (Coogan & Gillis 2013).
2. Sedimentary organic carbon accumulated in the continental environment and on the seafloor. This flux is of the order of 0.1 GtC/year (Lenton et al. 2018).

The residence time of carbon (the carbon content of a system divided by the sum of the output fluxes, at steady state) within the surficial Earth system is close to 150,000 years, a much longer timescale compared to the time required to mix the surficial Earth reservoirs. However, although 150,000 years might appear to be a long time period, it is short enough to allow huge fluctuations of the surficial Earth system at the geological timescale. Indeed, within a million years, the surficial Earth carbon reservoir can be renewed at least 6 times. In other words, a persistent difference of only 0.1 GtC/year between the global output flux and global input flux could cause Earth's surficial carbon stock to fall to zero within 400,000 years, with dramatic consequences for life on Earth. Compared to the hundreds of million years of the Phanerozoic (the past 539 million years of Earth history), 400,000 years is a short duration. It is also worth remembering that human activities release around 10 GtC/year into the atmosphere, which is huge compared to the geological carbon cycle disequilibria that is discussed in this contribution.

The consequences of this short residence time on the evolution of Earth's surficial environment have been identified by Garrels & Perry (1974) and nicely illustrated by Westbroeck (1991). At the geological timescale, the carbon stock of the surficial Earth system is a tiny reservoir. This reservoir is subjected to geological forces, which may disequilibrate it in such a way that it could either be emptied or grow massively within 1 million years. Both cases would have disastrous consequences for the biosphere: a global-scale glaciation in the first case or the development of excessively high temperatures in the second. The persistence of life on the surface of the planet requires that the carbon content of the surficial Earth system is always close to the equilibrium state. Because the outgassing of the solid Earth is an external forcing to the surficial Earth system, the only solution is the existence of a sensitivity of the outflows of carbon to the carbon content itself, allowing for a negative feedback loop.

Fortunately, there is one process operating at Earth's surface that is able to stabilize the atmospheric CO₂ level and hence the climate: the chemical weathering of exposed silicate minerals. Once exposed to the physical conditions of Earth's surface, silicate minerals are not thermodynamically stable, causing them to dissolve. The dissolution is promoted by the presence of carbonic acid (from dissolved CO₂) in rainwater and in soil solutions. The dissolution reaction can be written as follows (showing dissolution of a plagioclase by carbonic acid, release of cations in the rivers, and precipitation of secondary clay mineral):



Although silicate rocks do not contain carbon, their dissolution generates alkalinity (e.g., HCO₃⁻), which is carried to the ocean by rivers, with the carbon coming from the atmosphere. When this alkalinity reaches the ocean, the saturation state of the ocean water with respect to carbonate minerals increases, generating an increase in calcium carbonate production by calcifying organisms to remove the alkalinity excess. In the above equation, two calcium ions are available for calcium carbonate precipitation and potential storage in the sediments. Each of those calcium ions takes with it 1 mole of carbon, originating from the atmosphere. Four are left behind in the ocean. It is therefore important to understand that the weathering of silicate rocks consumes CO₂ on geological timescales only if the process of calcium carbonate deposition in the oceans is functioning and can respond to the arrival of excess alkalinity.

3. FROM THE WALKER NEGATIVE FEEDBACK TO THE REAL WORLD: 40 YEARS OF DEBATE

As early as 1845, about 40 years before the first description of the greenhouse effect by Arrhenius (Maslin 2004), a French engineer named Ebelmen foresaw the need for some sort of coupling between the consumption of carbon dioxide by the alteration of rocks and its return via magmatic degassing, in order to stabilize the carbon cycle (Ebelmen 1845, Berner & Maasch 1996). It was only in 1981 that Walker and collaborators proposed the existence of a negative feedback reaction able to modulate the carbon cycle in order to stabilize the climate of Earth.

The Walker negative feedback is a simple and elegant model to explain the relative stability of Earth's climate. Walker et al. (1981) proposed the existence of a negative feedback allowing a control on the atmospheric CO₂ evolution in response to the increase of the solar constant (brightening of the Sun) from the time of Earth's formation 4.5 billion years ago to the present day. They explicitly stated that the time evolution of atmospheric CO₂ has also been impacted by other important factors, such as the paleogeography, the planetary albedo, and possible influence of

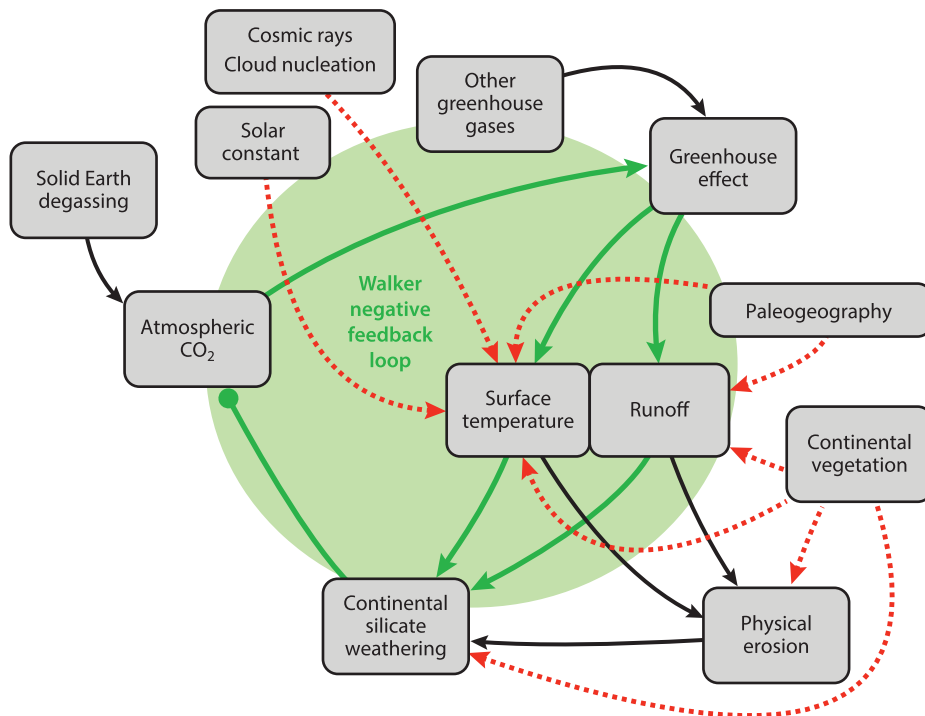


Figure 1

Overview of the feedback loop and causal links between the various components of the surficial Earth system. The green lines represent the silicate weathering negative feedback. A green arrow means a positive impact; a green dot represents a negative impact. The red arrows show the multiple connections between the various components of the geological evolution of Earth.

land plants on weathering rates. Walker et al. (1981) proposed the addition of a cog in a complex machine. They demonstrated that this additional cog is able to delay the evolution of Earth's surface temperature in response to the increase of the solar constant. They never claimed that this additional gear is the main controlling factor of the climate evolution of Earth. However, this feedback is nested in the core of the carbon cycle machinery and consequently plays a non-negligible role (**Figure 1**).

We can now state the two laws of the Earth-thermostat controlling the geological evolution of the carbon cycle:

1. The sum of the carbon fluxes leaving the surficial Earth system must always be very close to the carbon flux entering the surficial Earth system, to avoid lethal fluctuations.
2. To achieve this, negative feedbacks are required. The weathering of continental silicates can play this role. But there may be other solutions. It is worth mentioning that the existence of the silicate weathering feedback has been demonstrated from field data or data analysis at various timescales: from the decadal to the million years (Zeebe & Caldeira 2008, Gislason et al. 2009, Arnscheidt & Rothman 2022).

The first law cannot be violated because it is the mathematical consequence of the short residence time of carbon in the surficial Earth system, compared to the geological timescale. The second law is less constraining, and it allows us to consider new solutions rather than just the

climate-dependent silicate weathering. Most numerical models use a kind of Arrhenius type of equation to calculate the CO₂ consumption by silicate weathering (Dessert et al. 2001, Oliva et al. 2003):

$$F_{\text{silw}} = k \cdot \text{area} \cdot \text{runoff} \cdot e^{\left[\frac{-E_a}{R} \left(\frac{1}{T} - \frac{1}{298}\right)\right]}. \quad 1.$$

This law has been calibrated on field measurements. E_a is an apparent activation energy, generally around 40,000 J/mol. R is the ideal gas constant. Considering the data from which this equation has been calibrated, T is the mean annual temperature at the surface (in K), and runoff is the mean annual runoff (precipitation – evapotranspiration). k is a calibration constant that is fixed to fit the data. Area represents the surface of the considered continental zone: It could be the surface of a small watershed but also the surface of the continents. Given that runoff and temperature are functions of the atmospheric CO₂, this equation can be also written as a function of the CO₂ partial pressure (Caves-Rugenstein et al. 2019):

$$F_{\text{silw}} = k \cdot \text{area} \cdot R_{\text{CO}_2}^n, \quad 2.$$

where R_{CO_2} is the past partial pressure of CO₂, normalized to the preindustrial value.

4. NUMERICAL MODELS

We build numerical models when the system of interest is too complex to predict its evolution in response to external or internal changes. Numerical models are also a powerful method to evaluate the relative importance of a specific process within the carbon cycle. In this contribution, we focus only on models integrating the coupled evolution of the climate and of the carbon cycle (potentially coupled to other biogeochemical cycles) over geological timescales.

All these models belong to a category called box models. A box model decomposes the Earth system into a variable number of boxes connected to each other by flows of chemical species. The boxes are assumed to be well mixed and homogeneous. The number and the size of the boxes depend on the spatial and temporal scale of the study. This type of model allows for very long simulations, with simulated times easily exceeding 1 million years.

In a box model, the time evolution of a given reservoir i containing C_i moles of carbon (for instance, the carbon content of the atmosphere) is the solution of the mass balance between the input F_i^{in} and the output F_i^{out} fluxes. All these fluxes may be a function of time and a function of the size of one or several of the n simulated reservoirs:

$$\frac{dC_i}{dt} = F_i^{\text{in}}(t, C_1, \dots, C_n) - F_i^{\text{out}}(t, C_1, \dots, C_n). \quad 3.$$

The system is said to be at steady state when all the time derivatives are equal to zero, meaning that the input of elements to a given reservoir equals the output.

For the present discussion, we consider a simplified system with two boxes: one box with a short residence time (7 years), similar to the residence of carbon in the atmosphere, and one with a longer residence time (500 years), close to that of the ocean (**Figure 2**). We denote the short residence time reservoir as atmosphere and the other as LTSR (for Long residence Time Surficial Reservoir). These two boxes exchange carbon. We assume that these exchange fluxes are proportional to the size of the reservoir from which the fluxes come, while the fluxes entering a given reservoir do not depend on the carbon content of that reservoir. At steady state, the inverse of the proportionality constant is equal to the reaction time of the reservoir relative to the considered flux. In addition, the reservoir with the shorter residence time is fed by a geological flux (if this reservoir is the atmosphere, the geological flux can be the solid Earth degassing, for instance).

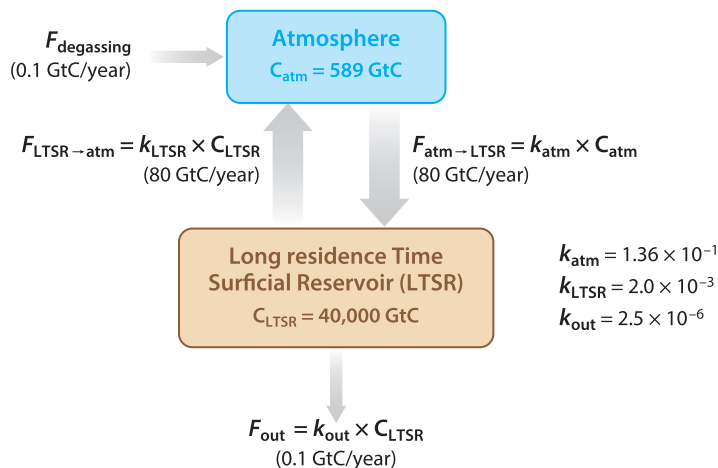


Figure 2

A schematic description of a simple 2-box model. C_{atm} and C_{LTSR} are the atmospheric content of carbon, and the amount of carbon stored in a Long residence Time Surficial Reservoir, respectively. All the exchange fluxes are assumed to be proportional to the reservoir where they come from. The k are the proportionality constants. $F_{\text{degassing}}$ is a forcing flux, such as the solid Earth degassing. F_{out} is a flux leaving the surficial reservoirs and transferring carbon to very long-term storage, such as the oceanic sediments. This theoretical model is used here as an illustration of the key role played by the residence times. This should not be considered as a careful representation of the carbon cycle.

For this experiment, we set this geological flux at 0.1 GtC/year. To avoid accumulation of carbon inside the two connected reservoirs, we also add an output flux that may potentially be interpreted as the sedimentary sink of carbon. This flux is set proportional to the size of the LTSR. At steady state, this flux is equal to 0.1 GtC/year. Our simple model is not a realistic simulation of the real world, but the conclusions we draw from it are generally applicable.

The system is first assumed to be at steady state, meaning that the content of carbon in the two reservoirs is constant through time, with the input flux of each reservoir balanced by the output flux. Then, we impose on the system a progressive rise in the outgassing of carbon, from its background value of 0.1 GtC/year to 0.15 GtC/year. Such an increase is far from being negligible: From the available reconstructions of the past degassing rate of the solid Earth, an increase by 50% never occurred in less than at least a few million years (Godd ris & Donnadi u 2019).

When this rise in degassing occurs within a human timescale of 50 years, the maximum disequilibrium in the content of carbon of the atmosphere is calculated at 0.008 GtC/year, while the LTSR disequilibrium culminates at 0.049 GtC/year, which is 10% of the increase in the degassing rate. Those values rapidly decrease to 0.00006 GtC/year and 0.004 GtC/year when the change in the outgassing occurs at a geological timescale of 5 million years. The last value is less than 1% of the change itself.

Based on these calculations, a useful simplification is to set the derivatives of the surficial reservoir to zero when simulating the evolution of the carbon cycle at the geological timescale. This assumption allows us to change the differential equations describing the evolution of the carbon cycle at the geological timescale into a set of simple algebraic equations. This simplification is applied in several models, such as GEOCARB and its later versions (Berner 2004, 2006) (Table 1).

A full demonstration of the validity to set the derivatives to zero, as long as the forcings are geological, can be found in the appendix by Fran ois & Godd ris (1998), based on a realistic representation of the carbon and alkalinity cycles.

Table 1 Brief overview of the models coupling the biogeochemical cycles to climate at the geological timescale

Model	Reference (nonexhaustive) ^a	Timescale (years)	Steady-state carbon cycle	Climate model	Geochemical model type	Modeled cycle(s)
BLAG	Berner et al. 1983	10^7 – 10^9	No	No climate model; global temperature is a parametric function of CO ₂ , and runoff is a parametric function of temperature	Single ocean-atmosphere box	Carbon, calcium, magnesium, alkalinity
GEOCARB	Berner 2004	10^7 – 10^9	Yes	No climate model; global temperature is a parametric function of CO ₂ , and runoff is a parametric function of temperature	Single ocean-atmosphere box	Carbon
GEOCARBSULF	Berner 2006	10^7 – 10^9	Yes	No climate model; global temperature is a parametric function of CO ₂ , and runoff is a parametric function of temperature	Single ocean-atmosphere box	Carbon, sulfur
GEOCARBSULFOR	Krause et al. 2018	10^5 – 10^9	No	No climate model; global temperature is a parametric function of CO ₂ , and runoff is a parametric function of temperature	Single ocean-atmosphere box	Carbon, sulfur
COPSE (Carbon, Oxygen, Phosphorus, Sulphur and Evolution)	Lenton et al. 2018	10^5 – 10^9	No	No climate model; global temperature is a parametric function of CO ₂ , and runoff is a parametric function of temperature	Single ocean-atmosphere box	Carbon, oxygen, phosphorus, nitrogen, sulfur, strontium, simplified calcium; alkalinity cycles in some versions
SCION (Spatial Continuous Integration)	Mills et al. 2021	10^5 – 10^9	No	Spatialized temperature and runoff fields on the continents	Single ocean-atmosphere box	Carbon, oxygen, phosphorus, nitrogen, sulfur, strontium
GEOCLIM	Maffre et al. 2022	10^3 – 10^6	No	Spatialized temperature and runoff fields on the continents	9-box ocean model and 1 atmospheric box	Carbon, alkalinity, phosphorus, oxygen, calcium, carbon and strontium isotopes
LOSCAR (Long-term Ocean-atmosphere Sediment Carbon Reservoir)	Zeebe 2012	10^3 – 10^6	No	No climate model; temperature is a parametric function of CO ₂	10+ ocean boxes depending on scenario and 1 atmospheric box	Carbon, alkalinity, phosphorus
MAGiC	Arvidson et al. 2006	10^5 – 10^9	No	No climate model; global temperature is a parametric function of CO ₂ , and runoff is a parametric function of temperature	Single ocean-atmosphere box	Carbon, calcium, magnesium, potassium, sulfur, phosphorus, oxygen, iron
REDBIO	Wallmann et al. 2019	10^3 – 10^6	No	No climate model; global temperature is a parametric function of CO ₂ , and runoff is a parametric function of temperature	6 ocean boxes and 1 atmospheric box	Oxygen, nitrogen, phosphorus, iron, sulfur, carbon, alkalinity

^aWe choose to cite only one reference per model.

5. THE RAYMO TURNING POINT

Based on the Earth-thermostat principle, Berner et al. (1983) built the first numerical model able to calculate the evolution of atmospheric CO₂ levels over the past 100 million years. This model was later termed BLAG after the authors' surnames, and it incorporates the negative feedback of silicate weathering. The BLAG model was mainly driven by the CO₂ outgassing input of carbon into the surficial Earth system. The role of silicate weathering was limited to a stabilization process able to limit the changes caused by variations in the outgassing rate. Although the role of silicate weathering is crucial, it is rather passive within this source-driven framework.

But the hypothesis that the carbon cycle is mainly driven by the sources of carbon was challenged in the late 1980s and early 1990s. Maureen Raymo and coauthors published several articles that can be seen as a turning point in our understanding of the geological evolution of the carbon cycle (Raymo et al. 1988, Raymo 1991). The reasoning of Raymo and colleagues is based on the carbonate sediment record of the ⁸⁷Sr/⁸⁶Sr ratio in seawater (Veizer et al. 1999). This record was first published in 1982 by Burke and coauthors (1982). A more recent version is available by Veizer et al. (1999), and compilations continue to add detail (McArthur et al. 2020), yet the fundamentals of the Cenozoic curve are unchanged. The most salient pattern in this curve is a steep rise over the past 40 million years or so. Because strontium has a high isotopic ratio in continental rocks and a low ratio in hydrothermal sources, Raymo (1991) concluded that this isotopic signal is a record of rapidly increasing chemical weathering of the continents, in the face of hydrothermal processes that remain at a low level. This rapid increase is attributed to the uplift of the Himalayas and the Tibetan plateau. Increasing slopes and decreasing temperatures with altitude promote physical erosion. A more fragmented rock presents a larger contact surface to the circulating fluids, which accelerates the dissolution of minerals and thus the consumption of CO₂. Tectonic uplift increases the global silicate weathering rate, consuming CO₂, cooling the climate, and favoring the onset of glaciers in some regions. Those glaciers will, in turn, increase the overall physical erosion of the continents, further consuming CO₂. But this hypothesis breaks the first law of the Earth-thermostat. Indeed, it introduces a positive feedback between climate cooling and silicate weathering. And when the first law is no longer applicable, with sinks greater than sources, CO₂ would disappear in a few million years, leading to extreme cooling and potentially a snowball glaciation.

When considering the intense debates of this period, it is clear now that there was a misunderstanding of the functioning of Walker's theory. The existence of a positive feedback loop within the carbon cycle does not exclude the presence of a negative loop. The two loops will interact, one destabilizing the climate, the other rebalancing it. The relative effectiveness of these two loops will allow for greater or lesser fluctuations in atmospheric CO₂ content and climate. Thus, nothing prevents erosion from increasing locally in response to tectonics, nor alteration from decreasing in other regions of the world as a result of global cooling (Godd ris & Fran ois 1995). The negative feedback loop, despite tectonic forcing working to destabilize it in some regions, has the ability to maintain the global flux of CO₂ consumption by silicate weathering at a level close to volcanic degassing. If degassing remained constant over the Cenozoic, as suggested by some reconstructions, then the global flux of weathering should also remain constant.

6. WEATHERING AND WEATHERABILITY

How can silicate weathering change the partial pressure of CO₂ if the sink of carbon through weathering must be close to the degassing rate? The answer is by changing the weatherability. The concept of weatherability was defined by Kump & Arthur (1997, p. 422). It is "the product of factors that affect rock chemical weathering other than climatic factors" (e.g., air temperature

and runoff). As reported by Caves et al. (2016), the dependence of the global silicate chemical weathering on atmospheric CO₂ can be expressed as a power function of the CO₂ level:

$$F_{\text{silw}} = kR_{\text{CO}_2}^n. \quad 4.$$

n ranges from 0.2 to 0.6 in most models [e.g., LOSCAR (Long-term Ocean-atmosphere Sediment Carbon Reservoir) (Zeebe 2012), GEOCARB (Berner 2004), COPSE (Carbon, Oxygen, Phosphorus, Sulphur and Evolution) (Bergman et al. 2004, Lenton et al. 2018)]. R_{CO_2} is the ratio between the CO₂ level at any time in the past and its present-day value. The power function should account for all the direct climatic effects (impact of temperature and runoff changes on silicate weathering, which both depend on the atmospheric CO₂ level). k is the weatherability. Given that the carbon cycle must be close to its steady state, we can write

$$F_{\text{vol}} = F_{\text{silw}}. \quad 5.$$

Combining Equations 4 and 5, we get the following simple relationship:

$$F_{\text{vol}} = kR_{\text{CO}_2}^n. \quad 6.$$

If the solid Earth degassing rate F_{vol} is known as a function of time, if k is known, and if n can be constrained, this simple equation can be solved to calculate the atmospheric CO₂ level. This equation is present in some form in models such as GEOCARB, LOSCAR, MAGic (Arvidson et al. 2006), and COPSE. Although this mathematical relationship is simple, it includes a large number of complex processes. n can fluctuate with age, depending on vegetation cover, for example. The weathering constant k depends on the presence or absence of mountain ranges. Finally, the rate of degassing of the solid Earth remains difficult to constrain in the past (Godd ris & Donnadieu 2019).

In summary, with respect to the evolution of Earth's climate during the Cenozoic, the uplift of large mountain ranges (such as the Himalayas) can modify the ability of rocks to weather under the effect of physical erosion, which increases with the presence of slopes, glaciers, and freeze-thaw alternation. Many authors have proposed an increase in the weatherability of continental surfaces (k) as the cause of the decrease in CO₂ content over the same period. The central question is then by how much weatherability increased over the past 40 million years. The simplest way to evaluate this is to use reconstructions of sedimentary masses accumulated on the seabed from the erosion of continents (Wold & Hay 1990), but this is still a rough method. It is obvious that the weatherability did not change at the same time and with the same amplitude everywhere on the continents. Some regions were affected by uplift but not the global surface as a whole. Although a simple model's response to the global increase in physical erosion will be quite strong and unequivocal, this method is not entirely convincing. The seawater ⁸⁷Sr/⁸⁶Sr record has also been used to constrain the physical erosive impact on k in GEOCARB (Berner 2006).

7. WEATHERABILITY AND ISOTOPIC SIGNALS

The short residence time of carbon in the surficial Earth system implies that silicate weathering rates remain close to solid Earth CO₂ emissions. If this degassing rate stayed roughly constant, then so should the silicate weathering flux. But if these fluxes were indeed both roughly constant, how can we explain the rise in the ⁸⁷Sr/⁸⁶Sr of the seawater over the past 40 million years? The answer here came from field measurements and models (Edmond 1992, Godd ris & Fran ois 1995, Galy & France-Lanord 1999): What is changing over the Cenozoic is not the global Sr flux generated by continental weathering but its isotopic signature. Highly radiogenic rocks are exposed in the Himalayas, and their dissolution brings radiogenic strontium to the ocean, forcing the oceanic ⁸⁷Sr/⁸⁶Sr to rise, while the global silicate weathering flux may stay constant.

A similar ubiquity can be suspected in the interpretation of the $^7\text{Li}/^6\text{Li}$ of the ocean, although this is more complex because of the fractionation of lithium isotopes during secondary phase precipitation. This fractionation implies that the riverine signature is dependent on the clay precipitation efficiency and is not strictly a signature of the rocks being weathered, as is the case for Sr. But again, the $^7\text{Li}/^6\text{Li}$ of the ocean can be explained by a change in the riverine $^7\text{Li}/^6\text{Li}$ together and/or a change in the weathering flux itself (Misra & Froelich 2012). Once the Li cycle coupled to the carbon mass balance, several combinations are consistent with the rise in seawater $^7\text{Li}/^6\text{Li}$: increasing riverine $^7\text{Li}/^6\text{Li}$ together with a decreasing Li flux or the reverse (Vigier & Godd eris 2015).

A constancy of global weathering has been suggested for the past 12 million years of the Cenozoic, based on the relatively constant $^9\text{Be}/^{10}\text{Be}$ ratio of marine sediments (Willenbring & Von Blanckenburg 2010). It was not correctly interpreted, as Willenbring & Von Blanckenburg (2010) concluded that silicate weathering rates were constant and therefore not the driver of Cenozoic climate cooling. But Caves Rugeinstein et al. (2019) took up this discussion and correctly interpreted that the constancy of the Be signal was a signal of constant global alteration, in a context of increasing weatherability.

8. SPATIALIZATION

A striking feature of most numerical models simulating climate and CO_2 evolution at the geological timescale is that they do not account for spatialization—the difference in processes across different parts of the land surface. These are mostly global-scale models, and they consider continental weathering as a single global value, driven by a mean global temperature and a mean global runoff (e.g., in GEOCARB, LOSCAR, and COPSE), and by global weatherability. A posteriori, this methodology may appear surprising, given that many mathematical relationships included in these models are nonlinear functions of the climatic parameters. This is critical when considering the climatic parameters of importance for silicate weathering. In the global-scale models, if CO_2 rises, global average temperature will also rise, as will global runoff. The continents are simulated as a single grid element, where silicate weathering can increase with CO_2 , only if weatherability is held constant. But the real world response of runoff to a change in CO_2 is highly complex. Globally, runoff will probably increase with atmospheric CO_2 . But locally, it may decrease, and this will be dependent on the local relief. Another important factor is the paleogeography—the positioning of the continents on Earth’s surface. The global runoff pattern will be strongly influenced by changes to paleogeography.

The first attempts to include spatialization of climate and silicate weathering in deep-time models of the carbon cycle date back to the late 1980s. Marshall et al. (1988) used an Energy Balance Model (EBM) to simulate the climate that divided Earth into latitudinal bands. The principle was to simulate climate variations as a function of latitude. The weathering rates were then calculated in each latitude band and summed to produce a global value. Using a climate model of the same type, Fran ois et al. (1993) built a numerical model coupling the global cycle of carbon, oxygen, phosphorus, and alkalinity to an EBM with 18 latitudinal bands. This work represented a significant advance in our understanding of the global evolution of Earth’s surface environment. It is worth keeping in mind that, during the same period, GEOCARB II was still using very simple laws linking global air temperature and global runoff, respectively, to the atmospheric CO_2 partial pressure and the global average temperature (Bernier 1994). However, despite this improvement of the calculation of the climatic fields using a more mechanistic model, EBMs do not resolve the water cycle. Fran ois et al. (1993) developed an equation allowing them to calculate the runoff for each latitudinal band as a function of the latitude and the calculated air temperature.

Taking a further step in this direction, Donnadiu et al. (2006) coupled a dynamic model of the main biogeochemical cycles (ten boxes, one of which describes the atmosphere and the other nine the ocean) to a General Circulation Model (GCM)-type climate model. An Atmospheric General Circulation Model (AGCM) is a complex numerical model describing the transport of matter and energy in the atmosphere in three dimensions. AGCMs can be coupled to a simple representation of the surface ocean that simulates the transport of heat as a diffusive process only—called a slab ocean. A more complete physical representation of the ocean can also be implemented, with diffusion and transport of heat and matter within the ocean. These models are called Atmosphere-Ocean General Circulation Models (AOGCMs). They include a physical representation of the water cycle and can be used to calculate continental runoff on a 2D-spatial grid covering the continents, together with the spatially resolved air temperature.

The model developed by Donnadiu et al. (2006) is called GEOCLIM, and it has been used for a large variety of studies. It was found that supercontinental configuration (for example, the Pangaea supercontinent that existed during the later Paleozoic and into the Mesozoic) would strongly limit the impact of changes to CO₂ on continental runoff because of the development of arid conditions over large continental surfaces. These periods are thus characterized by high steady-state CO₂ levels. Conversely, a wide dispersion of the continents should facilitate an increase of runoff with CO₂ (Godd ris et al. 2014). In addition to this, the climate sensitivity to atmospheric CO₂ (e.g., global warming per doubling of CO₂ concentration) is dependent on the continental configuration, ranging from about 4° for a CO₂ doubling during times of supercontinental configuration, or when large continental masses are located on the South Pole (such as in the early Paleozoic), to 2° for the present-day configuration. Finally, still using GEOCLIM, Godd ris & Donnadiu (2019) found that the paleogeographic control of the evolution of the carbon cycle and the climate is more pronounced in the Paleozoic. In the Mesozoic and Cenozoic, the continental dispersion appears to be large enough to force the Earth system into a glacial stage since the breakup phase of Pangaea in the Jurassic. As this was not the case, higher solid Earth degassing is required to keep CO₂ at a high level, especially during the Cretaceous.

Following the method employed in GEOCLIM, the SCION (Spatial Continuous Integration) model (Mills et al. 2021) extends the COPSE global biogeochemical model (which itself is a modification of GEOCARB) to include a spatial land surface informed by the FOAM GCM, which is interpolated over time as the continental configuration changes. The effects of continental distribution on the modeled atmospheric CO₂ evolution are similar to those observed in GEOCLIM, and the model predicts higher CO₂ levels during the time of the Pangaea supercontinent when compared to COPSE. An advantage of this new model is that the continuous whole-Phanerozoic simulations typical of COPSE and GEOCARB can now be run using a spatial representation of climate.

Adding a 2D representation of the continental surfaces allows for the simulation of the weathering fluxes accounting for the lithology. Richey et al. (2020) explored the sensitivity of the late Paleozoic climate to the spatially distributed weathering of mafic outcrops of variable size. Park et al. (2020) simulated the past 15 million years of global carbon cycle evolution, accounting for the presence of ultramafic rocks outcropping in a humid tropical Southeast Asia. Using an improved version of GEOCLIM, they found that the weathering of these ultramafic rocks is responsible for a global cooling of 3°C since 15 million years ago (Park et al. 2020). Reconstructing lithology further back into deep time becomes more challenging. At least large igneous provinces (LIPs) can be located on a map and assigned a lithological class (basalts). This has been done for the entire Cenozoic (Lefebvre et al. 2013) and for the late Proterozoic (Godd ris et al. 2017b). In both cases, the LIP weathering left its mark on the climatic evolution of Earth by reducing atmospheric CO₂

concentration during times when LIPs were exposed. Smaller and high-latitude LIPs such as the ~15 Ma Columbia River Basalt Group, however, were found to have a negligible effect on global silicate weathering [e.g., as explored in the SCION model (Longman et al. 2022)].

9. VEGETATION

The role of continental vegetation has been included in numerical models of the deep-time carbon cycle mainly because of biotic impacts on silicate weathering rates. Studies of the weathering processes in modern environments have shown that the presence of plants may increase weathering rates due to the belowground accumulation of CO₂, the release of organic acids, and the mechanical effect of roots (Drever 1994, Moulton et al. 2000, Porder 2019). This biological enhancement of global weathering reactions has been added in numerical models of the deep-time carbon cycle by modifying the weatherability factor. In nondimensional models, such as GEOCARB, the weatherability constant k is divided by 4 prior to the advent of land plants (representing the average effect seen in field studies). In the GEOCARB model (Bernier 1994), such a drastic decrease in the weatherability constant generates very high CO₂ levels in the early Paleozoic. To avoid this, a direct dependence of global weathering rates on atmospheric CO₂ was added, which was suggested to simulate the effect of the lower pH of rainwater (Bernier 2004).

GEOCARB-type models do not account for the change in hydrology associated with plant colonization of the land because they do not resolve the water cycle explicitly. Ibarra et al. (2019) built a cascade of models: a 1D model of water vapor transport feeding a reactive transport model for weathering to simulate the impact of the rise of the vascular plants in the Devonian. They found that the colonization of the continents by vascular plants has increased the global weatherability by a factor of about 2, with half of this increase being related to the hydrological effect triggered by the enhanced transpiration on the continents, allowing water vapor to be transported further into dry continental interiors.

Le Hir et al. (2011) used GEOCLIM coupled to a dynamic vegetation model to explore the global changes during the progressive colonization by vascular plants during the Devonian. This study was performed without accounting for a direct weatherability increase. The objective was to quantify the impact of plant-driven changes in the continental albedo, rugosity, and evapotranspiration on the global water cycle. They found that the decrease in albedo warms the continents enough to significantly increase the continental runoff. This change in runoff promotes weathering reactions, reducing the partial pressure of atmospheric CO₂. The calculated drop in CO₂ was from 7,000 ppm to 2,000 ppm between the Early and Late Devonian. Surprisingly, the air temperature at ground level remained about constant at around 22°C, the cooling generated by the CO₂ decrease being compensated for by the decrease in albedo.

There are currently no modeling studies that incorporate a dynamic, spatially resolved terrestrial biosphere evolving through the Paleozoic Era that also include the direct effect of a weatherability increase. Although the SCION model uses a spatially resolved climate (from GEOCLIM) and imposes a global weatherability increase due to plant evolution (like COPSE and GEOCARB), the weatherability change is simply applied to every continental grid cell regardless of habitability for plants. Future work will aim to link a dynamic global vegetation model (e.g., Gurung et al. 2022) in a similar manner to that of Le Hir et al. (2011).

Finally, Maffre et al. (2022) explored the impact of the plant colonization process on physical erosion and chemical weathering. They generated several random scenarios for the colonization phase. When a grid cell is colonized by vascular plants, chemical weathering increases and physical erosion is also impacted, either decreasing or increasing. They found that some scenarios generate a gentle CO₂ decrease, as continents are being progressively colonized. But other scenarios

generate first an ample increase of atmospheric CO₂. This is specifically the case for scenarios where the plants decrease physical erosion, promoting the growth of the regolith, which prevents the percolating water reaching the bedrock (see the next section).

There is currently a major effort to build process-based models of paleo-plants function to explore the interaction between ancient plants and their environments (Matthaeus et al. 2023). Once integrated into coupled ecological-climate models, these tools pave the way toward the reconstruction of the interaction between plants and climates in deep time. Those models are currently restricted to snapshot simulations.

10. EROSION

Since the early 2000s, the question of a possible control of the chemical weathering of rocks by physical erosion became increasingly widespread. From the field point of view, there is clearly a correlation between physical erosion and silicate rock weathering, as shown by Millot et al. (2002) and West et al. (2005). Several theoretical models have been developed (Gabet & Mudd 2009, West 2012, Maher & Chamberlain 2014). Those models focus on the silicate weathering sensitivity to climate, under various climatic conditions. For instance, Maher & Chamberlain (2014) showed that the sensitivity of silicate weathering to climate change is higher in areas where the residence time of water in soils is low (e.g., mountainous areas). Gabet & Mudd (2009) built a numerical model of weathering that includes the role of the thickness of the saprolite—a major contribution. Indeed, when thinking of physical erosion, we focus on places where this physical erosion is massive, such as in young and active mountain ranges (for instance, in Taiwan or New Zealand). As a result, a biased picture of continental surfaces seems to emerge from these studies in highly erosive areas. Outside of those regions, the continents look like vast flat surfaces where nothing happens.

However, the flat areas are indeed characterized by low weathering efficiency (low weatherability) because the saprolite is so thick that water cannot reach the fresh mineral at the saprolite-bedrock interface. Such systems are transport limited because the dissolution rates and the transport of solutes are limited by the capacity of the water to find its way into thick soil cover, typical of flat tropical environments. Using a coupled model describing physical erosion and weathering with a 2D spatial resolution, Carretier et al. (2014) showed that these flat areas weather 5 to 100 times slower than active orogens. Considering the present-day geography and the extent of flat areas, it is possible that flat areas consume as much CO₂ as the active orogens. But this needs to be explored. Also, for some large watersheds, the eroding mountains can provide fine-grained materials, without dissolving them, because the temperature is too low and because the residence time of water is too short. Those erosion products are then transported into the floodplains, where the temperature and runoff conditions promote weathering. This is the case in the Amazon, for example, where 50% of the CO₂ consumption occurs in the Andes, while the remaining 50% occurs in the floodplains (Moquet et al. 2011).

Up to now, the integration of physical erosion in large timescale box models such as GEOCARB or COPSE has been done by modifying the weatherability, with a corrective factor. As those models are global, lacking spatialization, this change in weatherability is applied to the entire continental surface. More importantly, the erosive factor is an external forcing parameter. This parameter is usually taken to be related to the total amount of sediments released in shallow seas over the Phanerozoic (Wold & Hay 1990). But physical erosion is not a forcing. Indeed, erosion is a function of the local slope but also of local climatic conditions (in particular runoff) (Syvitski & Milliman 2007).

Goddéris et al. (2017a), for the first time, accounted for physical erosion in the global-scale numerical model GEOCLIM. Here, physical erosion is calculated over the spatially resolved

continental surfaces. The mass balance of the saprolites is calculated on each continental grid cell, depending on slope and runoff. The saprolites are removed at the surface by physical erosion and created at the bottom by the dissolution of the bedrock. The dissolution rate of bedrock is a function of runoff and temperature, as usual, but modulated by a function decreasing with the thickness of the saprolite. This function simulates the progressive shift from a weathering-limited to a transport-limited regime, when the thickness of the saprolites increases. The most important thing here is that the physical erosion is updated at each time step using the evolving climatic fields from a GCM. The main difficulty is the definition of the slopes for each grid cell, which is poorly constrained in the distant past but required for the calculation of physical erosion. According to Godd eris et al. (2017a), the slopes are fixed for each grid cell and calculated from a correlation between altitude and slope observed for the present day. The problem therefore becomes the knowledge of topographic height in the geological past, which remains to this day a real challenge.

11. THE NEW MOUNTAINS

Our understanding of the carbon balance of mountains has considerably evolved since the hypothesis of Raymo (1991). Two Copernican evolutions occurred, the first one in 1997 with the publication by France-Lanord & Derry (1997). From measurements of suspended solids in the Himalayan rivers and in sediments of the Bengal Fan, they showed that the very high erosion rates generate an extremely efficient burial of organic matter on the seafloor. This organic matter comes either from tropical forests that cover the southern foothills of the Himalayas or from marine primary production. This flux is estimated to store two to three times more carbon than the silicate weathering flux. Ten years later, Galy et al. (2007) came to the same conclusion.

The second revolution came in 2014. Torres et al. (2014) identified a new process particularly active in the Himalayas but that was initially identified by Spence & Telmer (2005) in Northwest Canada. In some mountainous areas, physical erosion exposes pyrite-rich outcrops. In contact with the atmosphere, the pyrites oxidize and release sulfuric acid. This acid causes the dissolution of carbonates, which releases carbon from the rock to the rivers, and ultimately the carbon from the rock degasses toward the atmosphere. From the point of view of this process, the physical erosion of mountain ranges could generate CO₂. Torres et al. (2016) identified the same mechanism in the Andes.

But the modeling community largely ignored this new process. It was included in the global box model COPSE (in Mills et al. 2014), but the close balance of pyrite weathering and pyrite burial that model maintained completely nullified any long-term effect on atmospheric CO₂. The absence of dynamic modeling of physical erosion prohibited more detailed calculation of the erosion fluxes that are a controlling factor for sulfuric acid release and for organic carbon burial. More recently, Maffre et al. (2021) simulated the release of sulfuric acid in mountain ranges, using GEOCLIM and its spatialized representation of weathering and physical erosion. In this theoretical study, they released reduced sulfur, which is oxidized and contributes to the dissolution of carbonate and silicate rocks. During the first stage of the numerical experiment, the dissolution of carbonates by carbonic acid releases CO₂, and the atmospheric CO₂ content rises. But this is only a transient effect. Because oxygen is efficiently consumed during the reaction, the shallow epicontinental seas become progressively less oxygenated, promoting organic carbon preservation. After a short period of elevated CO₂, its concentration decreases rapidly, after only a few million years, limiting the consequence of this process.

12. SOLID EARTH DEGASSING

The rate of CO₂ degassing from the solid Earth has been reconstructed in various ways over the Phanerozoic and tentatively into the Neoproterozoic. The question of the outgassing rate of

the solid Earth is critical: It is clear that this flux is a first-order factor in the evolution of the carbon cycle. But constraining its amplitude and its time evolution is still a major challenge. One of the problems encountered in the reconstruction of outgassing rates comes from the fact that the global flux is the result of the addition of several components. These include the degassing rate of oceanic ridges (Domeier & Torsvik 2019) and different types of subduction zone volcanism and metamorphism (Lee et al. 2015, McKenzie et al. 2016), as well as continental rifting (Brune et al. 2017).

The first reconstruction was performed by Gaffin (1987), who used the evolution of sea level over the whole Phanerozoic to calculate a volume of the mid-oceanic ridge systems, which tends to be higher when hydrothermal activity is intense. The CO₂ degassing curve was then assumed to be proportional to this activity. The results show globally high degassing in the early Paleozoic and middle Mesozoic. Conversely, the end Paleozoic and the Cenozoic are characterized by low degassing rates. Other methods rely on the inventories of consumed lithosphere at subduction zones (Engebretson et al. 1992) or on the reconstruction of seafloor production rates (Cogné & Humler 2008). Recently, attention has been focused on continental arc volcanism (McKenzie et al. 2016). Visually, the reconstruction of continental arc volcanism over the Phanerozoic seems to be in agreement with the climatic fluctuations of Earth. However, the time resolution of the reconstructed arc volcanism is still quite low. For instance, McKenzie et al. (2016) showed that arc volcanism was limited at the time of the late Paleozoic ice age, but only around the end of the glacial period, and consequently can be considered only as a contributor to the climate cooling but not as the initiator of the ice age. Goddérís & Donnadieu (2019) tested a set of curves proposed in the literature by using the reconstructed histories in the GEOCLIM model. This exercise clearly showed the major impact of degassing on the carbon cycle and the poor constraint on the global outgassing flux.

Recently Müller et al. (2022) published a new CO₂ degassing curve for the Mesozoic and Cenozoic based on full plate tectonic modeling and a method for estimating the carbon content of the downgoing slab. A crucial point in this study is the decoupling of the CO₂ flux released during accretion at ocean ridges from degassing by arc volcanism over the Cenozoic. Müller et al. (2022) demonstrated that this decoupling is related to increased carbonate sedimentation on the pelagic seafloor. Indeed, the biological evolution of calcifiers led to a shift in sedimentary carbonate accumulation sites from the continental shelves in the Mesozoic to the deep ocean floor during the Cenozoic. As a result, ever-larger masses of carbonates were driven into subduction zones, leading to an increase in the rate of carbon outgassing by arc volcanism, which increasingly dominates the outgassing flow. This transfer of carbonate sedimentation had been described as early as 1989 (Volk 1989) and anticipated as a means of compensating for the increased chemical weathering of silicate rocks associated with the uplift of the Himalayas and the Tibetan plateau (Caldeira 1992). This result is particularly interesting and challenges interpretation of the ⁹Be/¹⁰Be record, which was assumed to imply constant global silicate weathering. Given a rigorous 4D modeling approach, the full plate method can also be extended to include other sources of CO₂ such as the heating of overlying sediments in continental arcs (Lee et al. 2015) and CO₂ sources at rifts (Brune et al. 2017).

13. SEAFLOOR WEATHERING

The CO₂ consumption by the alteration of seafloor basalts in contact with seawater was first described in the early 1980s. This additional carbon flux is potentially an important process in the carbon cycle evolution (Isson et al. 2019). Like the weathering of continental rocks, this process releases alkalinity into the waters circulating inside the seafloor. This alkalinity is then removed from

the seawater via the precipitation of calcium carbonates in the seafloor (Staudigel & Hart 1983, Spivack & Staudigel 1994). Seafloor weathering was recognized early on as a significant carbon sink (Brady & Gislason 1997). The magnitude of the sink has been estimated at 0.02 GtC/year (Coogan & Gillis 2013), able to play a significant role in the geological evolution of the carbon cycle. François et al. (1993) developed a numerical model of the carbon cycle integrating the role of seafloor weathering in order to understand the evolution of climate over the Cenozoic, mainly based on the seawater $^{87}\text{Sr}/^{86}\text{Sr}$. The seawater $^{87}\text{Sr}/^{86}\text{Sr}$ has rapidly risen since about 40 million years ago, and this rise was first interpreted as a rapid increase in global silicate weathering (Raymo 1991). But as mentioned before, the sinks and sources of carbon must always be close to steady state. Through the introduction of seafloor weathering, the mass balance of the inorganic carbon cycle moves from

$$\text{solid Earth degassing} = \text{continental silicate weathering},$$

which is the first law of the Earth-paleothermostat, into the following expression:

$$\text{solid Earth degassing} = \text{continental silicate weathering} + \text{seafloor weathering}.$$

If the degassing rate stays constant, a way to increase the continental silicate weathering rate over the Cenozoic is to assume that seafloor weathering has decreased at the same time (Goddéris & François 1995). Because continental weathering provides radiogenic strontium to the ocean, while seafloor weathering and water-rock interaction at mid-oceanic ridges release less radiogenic strontium, the addition of seafloor weathering to the conceptual framework allows an increase in the strontium isotopic ratio of the ocean, without invoking a change in the isotopic composition of the source rocks.

But why would seafloor weathering rates be higher at the end of the Mesozoic compared to today? One possibility is that a higher ridge generation rate in the late Mesozoic allowed for high rates of seafloor weathering (e.g., Gillis & Coogan 2011, Mills et al. 2014). Brady & Gislason (1997) were the first to suggest a strong temperature dependence. Given that the temperature of the deep sea was 10 to 20°C above the present-day value, ocean floor basalts should dissolve faster. But a higher dissolution accompanied by a greater storage of carbonates inside the ocean crust might also be due to a different chemical composition of the oceans (especially the content of K) in the late Mesozoic. Le Hir et al. (2011) tried to account for this flux during the Snowball Earth glacial episode in the Neoproterozoic by simulating the dependence on pH and on the affinity of the seawater with respect to the minerals composing the oceanic crust. They found that seafloor weathering can strongly increase the duration of the total glaciation, given its efficiency under low pH conditions, and due to the accumulation of CO₂ in the surficial Earth system.

14. CONCLUSIONS

Many questions have been considered using numerical models of the long-term carbon cycle coupled to climatic simulation. But in the end, few of them have been answered definitively. A great suite of models exist (e.g., **Table 1**) that include different processes and operate over different timescales, usually with models that include more detailed processes also having a more limited timeframe of operation. This means that while meaningful conclusions have been drawn on carbon sources and sinks over Phanerozoic and later Neoproterozoic time, it has not been possible to include all of the relevant mechanisms (at appropriate resolution) into a single model.

We strongly believe that numerical models should be used to identify and quantify processes impacting the evolution of the carbon cycle and climate, and not as tools able to reconstruct

past environments precisely, for the simple reason that the complexity of nature cannot be fully integrated into a model. In addition, when going back into deep time, we have to acknowledge that most of the data have been lost forever. Short-term fluctuations progressively disappear from the record when going back in time because the time resolution decreases with geological age. Because of this decrease, it is almost certain that we are losing sight of the connections between short-term events and multimillion-year climate and carbon cycle evolution. Deep time should be considered as a timescale continuum, while the models generally consider only the long-term components alone.

Over the past 30 years, models have greatly improved our understanding of carbon cycle evolution. One of the most exciting research topics here has been the simulation of the role of land vegetation on the long-term evolution of the global carbon cycle and climate. Moving from basic corrections applied to the global silicate weathering rate, newer models now include the impact of land plants not only on weathering but also on surface rugosity, albedo, evapotranspiration, and physical erosion. The most recent models also now include ecological processes adapted to deep time, simulating the behavior of extinct species. Another important breakthrough is the ability to take into account the spatial resolution of processes, allowing researchers to spatially simulate, for example, the weatherability of the continental surfaces.

From the numerical models listed in **Table 1**, it seems to us that the historical trend has been to refine models that were initially quite coarse. Then, depending on the object of study, the oceanic part of the model may also be refined by increasing the number of oceanic reservoirs in the box model. One of the problems of this approach is the total absence of 3D ocean dynamics, which would react directly to CO₂ variations during the simulations. This leads us to a model that we have not discussed because it follows the opposite path: the GENIE (Grid ENabled Integrated Earth system) model (Ridgwell et al. 2007). Unlike the other models discussed in this review, GENIE is a dynamic ocean model that calculates the chemical composition of the water and the dynamics of ocean transport at the same time. But running GENIE over millions of years requires a very long computer run time. Using the $36 \times 36 \times 16$ ocean resolution, a 1 Myr model run took around two months to complete (Colbourn et al. 2015, Lord et al. 2016). This timeframe limitation is the reason why GENIE includes a rather coarse representation of the climate and a simplified description of the weathering processes. Regarding weathering, the GEOCLIM model includes the most mechanistic description of this process. But when models are refined, we rapidly lack data about the boundary conditions such as the topography of the continents in the past and the bathymetry of the seafloor.

So we have to keep in mind that some required information to constrain mechanistic models has disappeared forever. This may push modelers to experiment with a more stochastic method, generating uncertainties in the input data and boundary conditions, and performing ensembles of runs, instead of only one solution.

It is a tradition to end a review with some perspectives for future research. We anticipate exciting developments might depend on the following:

1. A better quantified CO₂ degassing flux, taking into account all of the different carbon releasing processes.
2. Clearer understanding of the terrestrial vegetation. To what degree does it enhance weathering directly versus indirectly, and what were the paleo-distributions of vegetation, and their interactions with the climatic parameters, including the water cycle?
3. Calculating the elemental budget of mountain ranges, accounting for all the processes that generate or sequester carbon.
4. Including the behavior of marine ecosystems into geological Earth system models.

DISCLOSURE STATEMENT

The authors are not aware of any affiliations, memberships, funding, or financial holdings that might be perceived as affecting the objectivity of this review.

ACKNOWLEDGMENTS

This revision has benefited from numerous and fruitful discussions with the members of the French Deep-Time Paleoclimate Modelling Group (<https://paleoclim-cnrs.github.io>).

LITERATURE CITED

- Arnscheidt CW, Rothman DH. 2022. Presence or absence of stabilizing Earth system feedbacks on different time scales. *Sci. Adv.* 8:eadc9241
- Arvidson RS, Mackenzie FT, Guidry M. 2006. MAGic: a Phanerozoic model for the geochemical cycling of major rock-forming components. *Am. J. Sci.* 306:135–90
- Barron EJ. 1983. A warm, equable Cretaceous: the nature of the problem. *Earth-Sci. Rev.* 19:305–38
- Bergman NM, Lenton TM, Watson AJ. 2004. COPSE: a new model of biogeochemical cycling over Phanerozoic time. *Am. J. Sci.* 304:397–437
- Berner RA. 1994. Geocarb II: a revised model of atmospheric CO₂ over Phanerozoic time. *Am. J. Sci.* 294:56–91
- Berner RA. 2004. *The Phanerozoic Carbon Cycle*. Oxford, UK: Oxford Univ. Press
- Berner RA. 2006. GEOCARBSULF: a combined model for Phanerozoic atmospheric O₂ and CO₂. *Geochim. Cosmochim. Acta* 70:5653–64
- Berner RA, Lasaga AC, Garrels RM. 1983. The carbonate-silicate geochemical cycle and its effect on atmospheric carbon dioxide over the past 100 million years. *Am. J. Sci.* 283:641–83
- Berner RA, Maasch KA. 1996. Chemical weathering and controls on atmospheric O₂ and CO₂: fundamental principles were enunciated by J. J. Ebelmen in 1845. *Geochim. Cosmochim. Acta* 60:1633–37
- Braconnot P, Otto-Bliesner B, Harrison S, Joussaume S, Peterchmitt J-Y, et al. 2007. Results of PMIP2 coupled simulations of the Mid-Holocene and Last Glacial Maximum—Part 1: experiments and large-scale features. *Clim. Past* 3:261–77
- Brady PV, Gislason SR. 1997. Seafloor weathering controls on atmospheric CO₂ and global climate. *Geochim. Cosmochim. Acta* 61:965–73
- Brune S, Williams SE, Muller RD. 2017. Potential links between continental rifting, CO₂ degassing and climate change through time. *Nat. Geosci.* 10:941–46
- Burke WH, Denison RE, Hetherington EA, Koepnick RB, Nelson HF, Otto JB. 1982. Variation of seawater ⁸⁷Sr/⁸⁶Sr throughout Phanerozoic time. *Geology* 10:516–19
- Caldeira K. 1992. Enhanced Cenozoic chemical weathering and the subduction of pelagic carbonate. *Nature* 357:578–81
- Carretier S, Godd ris Y, Delannoy T, Rouby D. 2014. Mean bedrock-to-saprolite conversion and erosion rates during mountain growth and decline. *Geomorphology* 209:39–52
- Caves JK, Jost AB, Lau KV, Maher K. 2016. Cenozoic carbon cycle imbalances and a variable weathering feedback. *Earth Planet. Sci. Lett.* 450:152–63
- Caves Rugenstein JK, Ibarra DE, Von Blanckenburg F. 2019. Neogene cooling driven by land surface reactivity rather than increased weathering fluxes. *Nature* 571:99–102
- Cogn  JP, Humler E. 2008. Global scale patterns of continental fragmentation: Wilson’s cycles as a constraint for long-term sea-level changes. *Earth Planet. Sci. Lett.* 273:251–59
- Colbourn G, Ridgwell A, Lenton TM. 2015. The time scale of the silicate weathering negative feedback on atmospheric CO₂. *Glob. Biogeochem. Cycles* 29:583–96
- Coogan LA, Gillis KM. 2013. Low-temperature alteration of the seafloor: impacts on ocean chemistry. *Annu. Rev. Earth Planet. Sci.* 46:21–45
- Dessert C, Dupr  B, Fran ois LM, Schott J, Gaillardet J, et al. 2001. Erosion of Deccan Traps determined by river geochemistry: impact on the global climate and the ⁸⁷Sr/⁸⁶Sr ratio of seawater. *Earth Planet. Sci. Lett.* 188:459–74

- Domeier M, Torsvik TH. 2019. Full-plate modelling in pre-Jurassic time. *Geol. Mag.* 156:261–80
- Donnadieu Y, Godd ris Y, Pierrehumbert R, Dromart G, Fluteau F, Jacob R. 2006. A GEOCLIM simulation of climatic and biogeochemical consequences of Pangea breakup. *Geochim. Geophys. Geosyst.* 7:Q11019
- Drever JL. 1994. The effect of land plants on weathering rates of silicate minerals. *Geochim. Cosmochim. Acta* 58:2325–32
- Ebelmen JJ. 1845. Sur les produits de la d composition des esp ces min rales de la famille des silicates. *Ann. Mines* 7:3–66
- Edmond JM. 1992. Himalayan tectonics, weathering processes, and the strontium isotope record in marine limestones. *Science* 258:1594–97
- Engelbreton DC, Kelley KP, Cashman HJ, Richards MA. 1992. 180 Million years of subduction. *GSA Today* 2:93–100
- France-Lanord C, Derry LA. 1997. Organic carbon burial forcing of the carbon cycle from Himalayan erosion. *Nature* 390:65–67
- Fran ois LM, Walker JCG, Opdyke BN. 1993. The history of global weathering and the chemical evolution of the ocean-atmosphere system. *Geophys. Monogr. Series* 74:143–59
- Fran ois LM, Godd ris Y. 1998. Isotopic constraints on the Cenozoic evolution of the carbon cycle. *Chem. Geol.* 145:177–212
- Gabet EJ, Mudd SM. 2009. A theoretical model coupling chemical weathering rates with denudation rates. *Geology* 37:151–54
- Gaffin S. 1987. Ridge volume dependence on seafloor generation rate and inversion using long term sealevel change. *Am. J. Sci.* 287:596–611
- Gaillardet J, Dupr  B, Louvat P, All gre CJ. 1999. Global silicate weathering and CO₂ consumption rates deduced from the chemistry of large rivers. *Chem. Geol.* 159:3–30
- Galy A, France-Lanord C. 1999. Weathering processes in the Ganges-Brahmaputra basin and the riverine alkalinity budget. *Chem. Geol.* 159:31–60
- Galy V, France-Lanord C, Beyssac O, Faure P, Kudrass H, Palhol F. 2007. Efficient organic carbon burial in the Bengal fan sustained by the Himalayan erosional system. *Nature* 450:407–9
- Garrels RM, Perry EH. 1974. Cycling of carbon, sulfur, and oxygen through geologic time. In *The Sea*, Vol. 5, ed. ED Goldberg, pp. 303–36. New York: Wiley-Interscience
- Gerlach T. 2011. Volcanic versus anthropogenic carbon dioxide. *Eos Trans. AGU* 92(24):201–2
- Gillis KM, Coogan LA. 2011. Secular variation in carbon uptake into the ocean crust. *Earth Planet. Sci. Lett.* 302:385–92
- Gislason SR, Oelkers EH, Eiriksdottir ES, Kardjilov MI, Gisladottir G, et al. 2009. Direct evidence of the feedback between climate and weathering. *Earth Planet. Sci. Lett.* 277:213–22
- Godd ris Y, Donnadieu Y. 2019. A sink- or a source-driven carbon cycle at the geological timescale? Relative importance of palaeogeography versus solid Earth degassing rate in the Phanerozoic climatic evolution. *Geol. Mag.* 156:355–65
- Godd ris Y, Donnadieu Y, Carretier S, Aretz M, Dera G, et al. 2017a. Onset and ending of the late Palaeozoic ice age triggered by tectonically paced rock weathering. *Nat. Geosci.* 10:382–86
- Godd ris Y, Donnadieu Y, Le Hir G, Lefebvre V, Nardin E. 2014. The role of palaeogeography in the Phanerozoic history of atmospheric CO₂ and climate. *Earth-Sci. Rev.* 128:122–38
- Godd ris Y, Francois LM. 1995. The Cenozoic evolution of the strontium and carbon cycles: relative importance of continental erosion and mantle exchanges. *Chem. Geol.* 126:169–90
- Godd ris Y, Le Hir G, Macouin M, Donnadieu Y, Hubert-Theou L, et al. 2017b. Paleogeographic forcing of the strontium isotopic cycle in the Neoproterozoic. *Gondwana Res.* 42:151–62
- Gurung K, Field KJ, Batterman SA, Godd ris Y, Donnadieu Y, et al. 2022. Climate windows of opportunity for plant expansion during the Phanerozoic. *Nat. Commun.* 13:4530
- Ibarra DE, Caves Rugenstein JK, Bachan A, Baresch A, Lau KV, et al. 2019. Modeling the consequences of land plant evolution on silicate weathering. *Am. J. Sci.* 319:1–43
- IPCC (Intergov. Panel Clim. Change). 2021. *Climate Change 2021: The Physical Science Basis. Contribution of Working Group I to Sixth Assessment Report of the Intergovernmental Panel on Climate Change*, ed. V Masson-Delmotte, P Zhai, A Pirani, SL Connors, C P an, et al. New York: Cambridge Univ. Press

- Isson TT, Planavsky NJ, Coogan LA, Stewart EM, Ague JJ, et al. 2019. Evolution of the global carbon cycle and climate regulation on Earth. *Glob. Biogeochem. Cycles* 34:e2018GB006061
- Krause AJ, Mills BJW, Zhang S, Planavsky NJ, Lenton TM, Poulton SW. 2018. Stepwise oxygenation of the Paleozoic atmosphere. *Nat. Commun.* 9:4081
- Kump LR, Arthur MA. 1997. Global chemical erosion during the Cenozoic: Weatherability balances the budgets. In *Tectonic Uplift and Climate Change*, ed. WF Ruddiman, pp. 399–426. New York: Springer US
- Le Hir G, Donnadieu Y, Godd ris Y, Meyer-Berthaud B, Ramstein G, Blakey RC. 2011. The climate change caused by the land plant invasion in the Devonian. *Earth Planet. Sci. Lett.* 310:203–12
- Lee CTA, Thurner S, Cao WR. 2015. The rise and fall of continental arcs: interplays between magmatism, uplift, weathering, and climate. *Earth Planet. Sci. Lett.* 425:105–19
- Lefebvre V, Donnadieu Y, Godd ris Y, Fluteau F, Hubert-Theou L. 2013. Was the Antarctic glaciation delayed by a high degassing rate during the early Cenozoic? *Earth Planet. Sci. Lett.* 371:203–11
- Lenton TM, Daines SJ, Mills BJW. 2018. COPSE reloaded: an improved model of biogeochemical cycling over Phanerozoic time. *Earth-Sci. Rev.* 178:1–28
- Longman J, Mills BJW, Donnadieu Y, Godd ris Y. 2022. Assessing volcanic controls on Miocene climate change. *Geophys. Res. Lett.* 49(2):e2021GL096519
- Lord NS, Ridgwell A, Thorne MC, Lunt DJ. 2016. An impulse response function for the “long tail” of excess atmospheric CO₂ in an Earth system model. *Glob. Biogeochem. Cycles* 30:2–17
- Maffre P, Godd ris Y, Pohl A, Donnadieu Y, Carretier S, Le Hir G. 2022. The complex response of continental silicate rock weathering to the colonization of the continents by vascular plants in the Devonian. *Am. J. Sci.* 322:461–92
- Maffre P, Swanson-Hysel NL, Godd ris Y. 2021. Limited carbon cycle response to increased sulfide weathering due to oxygen feedback. *Geophys. Res. Lett.* 48:e2021GL094589
- Maher K, Chamberlain CP. 2014. Hydrologic regulation of chemical weathering and the geologic carbon cycle. *Science* 343:1502–4
- Marshall HG, Walker JCG, Kuhn WR. 1988. Long-term climate change and the geochemical cycle of carbon. *J. Geophys. Res.* 93(D1):791–801
- Maslin M. 2004. *Global Warming: A Very Short Introduction*. Oxford, UK: Oxford Univ. Press
- Matthaeus WJ, Macarewhich SI, Richey J, Montanez IP, McElwain JC, et al. 2023. A systems approach to understanding how plants transformed Earth’s environment in deep time. *Annu. Rev. Earth Planet. Sci.* 51:551–80
- McArthur JM, Howarth RJ, Shields GA, Zhou Y. 2020. Strontium isotope stratigraphy. In *Geologic Time Scale 2020*, ed. FM Gradstein, JG Ogg, MD Schmitz, GM Ogg, pp. 211–38. Amsterdam: Elsevier
- McKenzie NR, Horton BK, Loomis SE, Stockli DF, Planavsky NJ, Lee CTA. 2016. Continental arc volcanism as the principal driver of icehouse-greenhouse variability. *Science* 352:444–47
- Millot R, Gaillardet J, Dupre B, Allegre CJ. 2002. The global control of silicate weathering rates and the coupling with physical erosion: new insights from rivers of the Canadian Shield. *Earth Planet. Sci. Lett.* 196:83–98
- Mills B, Daines SJ, Lenton TM. 2014. Changing tectonic controls on the long-term carbon cycle from Mesozoic to present. *Geochem. Geophys. Geosyst.* 15:4866–84
- Mills BJW, Donnadieu Y, Godd ris Y. 2021. Spatial continuous integration of Phanerozoic global biogeochemistry and climate. *Gondwana Res.* 100:73–86
- Misra S, Froelich PN. 2012. Lithium isotope history of Cenozoic seawater: changes in silicate weathering and reverse weathering. *Science* 335:818–23
- Moquet J-S, Crave A, Viers J, Seyler P, Armijos E, et al. 2011. Chemical weathering and atmospheric/soil CO₂ uptake in the Andean and Foreland Amazon basins. *Chem. Geol.* 287:1–26
- Moulton KL, West J, Berner RA. 2000. Solute flux and mineral mass balance approaches to the quantification of plant effects on silicate weathering. *Am. J. Sci.* 300:539–70
- M ller RD, Mather B, Dutkiewicz A, Keller T, Merdith A, et al. 2022. Evolution of Earth’s tectonic carbon conveyor belt. *Nature* 605:629–39
- Oliva P, Viers J, Dupr  B. 2003. Chemical weathering in granitic environments. *Chem. Geol.* 202:225–56

- Park Y, Maffre P, Godd ris Y, Swanson-Hysell NL. 2020. Emergence of the Southeast Asian islands as a driver for Neogene cooling. *PNAS* 117:25319–26
- Porder S. 2019. How plants enhance weathering and how weathering is important to plants. *Elements* 15:241–46
- Raymo ME. 1991. Geochemical evidence supporting T. C. Chamberlin’s theory of glaciation. *Geology* 19:344–47
- Raymo ME, Ruddiman WF, Froelich PN. 1988. Influence of late Cenozoic mountain building on ocean geochemical cycles. *Geology* 16:649–53
- Richey JD, Montanez IP, Godd ris Y, Looy CV, Griffis NP, DiMichele WA. 2020. Influence of temporally varying weatherability on CO₂-climate coupling and ecosystem change in the late Paleozoic. *Clim. Past* 16:1759–75
- Ridgwell A, Hargreaves J, Edwards N, Annan J, Lenton T, et al. 2007. Marine geochemical data assimilation in an efficient Earth system model of global biogeochemical cycling. *Biogeosciences* 4:87–104
- Spence J, Telmer K. 2005. The role of sulfur in chemical weathering and atmospheric CO₂ fluxes: evidence from major ions, $\delta^{13}\text{C}_{\text{DIC}}$, and $\delta^{34}\text{S}_{\text{SO}_4}$ in rivers of the Canadian Cordillera. *Geochim. Cosmochim. Acta* 69:5441–48
- Spivack AJ, Staudigel H. 1994. Low-temperature alteration of the upper oceanic crust and the alkalinity budget of seawater. *Chem. Geol.* 115:239–47
- Staudigel H, Hart SR. 1983. Alteration of basaltic glass: mechanisms and significance for the oceanic crust-seawater budget. *Geochim. Cosmochim. Acta* 47:337–50
- Syvitski JPM, Milliman JD. 2007. Geology, geography, and humans battle for dominance over the delivery of fluvial sediment to the coastal ocean. *J. Geol.* 115:1–19
- Tierney JE, Poulsen CJ, Montanez IP, Bhattacharya T, Feng R, et al. 2020. Past climates inform our future. *Science* 370:eaay3701
- Torres MA, West AJ, Clark KE, Paris G, Bouchez J, et al. 2016. The acid and alkalinity budgets of weathering in the Andes–Amazon system: insights into the erosional control of global biogeochemical cycles. *Geochim. Cosmochim. Acta* 450:381–91
- Torres MA, West AJ, Li GJ. 2014. Sulphide oxidation and carbonate dissolution as a source of CO₂ over geological timescales. *Nature* 507:346–49
- Veizer J, Ala D, Azmy K, Bruckschen P, Buhl D, et al. 1999. ⁸⁷Sr/⁸⁶Sr, $\delta^{13}\text{C}$ and $\delta^{18}\text{O}$ evolution of Phanerozoic seawater. *Chem. Geol.* 161:59–88
- Vigier N, Godd ris Y. 2015. A new approach for modeling Cenozoic oceanic lithium isotope paleo-variations: the key role of climate. *Clim. Past* 11:635–45
- Volk T. 1989. Sensitivity of climate and atmospheric CO₂ to deep-ocean and shallow-ocean carbonate burial. *Nature* 337:637–40
- Walker JCG, Hays PB, Kasting JF. 1981. A negative feedback mechanism for the long-term stabilization of Earth’s surface temperature. *J. Geophys. Res.* 86(C10):9776–82
- Wallmann K, Fl gel S, Scholz F, Dale AW, Kemena TP, et al. 2019. Periodic changes in the Cretaceous ocean and climate caused by marine redox see-saw. *Nat. Geosci.* 12:456–61
- West AJ. 2012. Thickness of the chemical weathering zone and implications for erosional and climatic drivers of weathering and for carbon-cycle feedbacks. *Geology* 40:811–14
- West AJ, Galy A, Bickle M. 2005. Tectonic and climatic controls on silicate weathering. *Earth Planet. Sci. Lett.* 235:211–28
- Westbroeck P. 1991. *Life as a Geological Force*. New York: W.W. Norton
- Willenbring JK, Von Blanckenburg F. 2010. Long-term stability of global erosion rates and weathering during the late-Cenozoic cooling. *Nature* 465:211–14
- Wold CN, Hay WW. 1990. Estimating ancient sediment fluxes. *Am. J. Sci.* 290:1069–89
- Zeebe RE. 2012. LOSCAR: Long-term Ocean-atmosphere-Sediment Carbon cycle Reservoir Model v2.0.4. *Geosci. Model Dev.* 5:149–66
- Zeebe RE, Caldeira K. 2008. Close mass balance of long-term carbon fluxes from ice-core CO₂ and ocean chemistry record. *Nat. Geosci.* 1:312–15

Contents

Estella Atekwana: Autobiographical Notes <i>Estella A. Atekwana</i>	1
The Evolving Chronology of Moon Formation <i>Lars E. Borg and Richard W. Carlson</i>	25
Harnessing the Power of Communication and Behavior Science to Enhance Society's Response to Climate Change <i>Edward W. Maibach, Sri Saabitya Uppalapati, Margaret Orr, and Jagadish Thaker</i>	53
River Deltas and Sea-Level Rise <i>Jaap H. Nienhuis, Wonsuck Kim, Glenn A. Milne, Melinda Quock, Aimée B.A. Slangen, and Torbjörn E. Törnqvist</i>	79
Machine Learning in Earthquake Seismology <i>S. Mostafa Mousavi and Gregory C. Beroza</i>	105
Bubble Formation in Magma <i>James E. Gardner, Fabian B. Wadsworth, Tamara L. Carley, Edward W. Llewellyn, Halim Kusumaatmaja, and Dork Sahagian</i>	131
Continental Crustal Growth Processes Recorded in the Gangdese Batholith, Southern Tibet <i>Di-Cheng Zhu, Qing Wang, Roberto F. Weinberg, Peter A. Cawood, Zhidan Zhao, Zeng-Qian Hou, and Xuan-Xue Mo</i>	155
Iceberg Calving: Regimes and Transitions <i>R.B. Alley, K.M. Cuffey, J.N. Bassis, K.E. Alley, S. Wang, B.R. Parizek, S. Anandakrishnan, K. Christianson, and R.M. DeConto</i>	189
Fracture Energy and Breakdown Work During Earthquakes <i>Massimo Cocco, Stefano Aretusini, Chiara Cornelio, Stefan B. Nielsen, Elena Spagnuolo, Elisa Tinti, and Giulio Di Toro</i>	217
Evolution of Atmospheric O ₂ Through the Phanerozoic, Revisited <i>Benjamin J.W. Mills, Alexander J. Krause, Ian Jarvis, and Bradley D. Cramer</i>	253

Instructive Surprises in the Hydrological Functioning of Landscapes <i>James W. Kirchner, Paolo Benettin, and Ilja van Meerveld</i>	277
Deconstructing the Lomagundi-Jatuli Carbon Isotope Excursion <i>Malcolm S.W. Hodgskiss, Peter W. Crockford, and Alexandra V. Turchyn</i>	301
Elastic Thermobarometry <i>Matthew J. Kohn, Mattia L. Mazzucbelli, and Matteo Alvaro</i>	331
Mimas: Frozen Fragment, Ring Relic, or Emerging Ocean World? <i>Alyssa Rose Rhoden</i>	367
The Mid-Pleistocene Climate Transition <i>Timothy D. Herbert</i>	389
Neogene History of the Amazonian Flora: A Perspective Based on Geological, Palynological, and Molecular Phylogenetic Data <i>Carina Hoorn, Lúcia G. Lobmann, Lydian M. Boschman, and Fabien L. Condamine</i>	419
Hydrological Consequences of Solar Geoengineering <i>Katharine Ricke, Jessica S. Wan, Marissa Saenger, and Nicholas J. Lutsko</i>	447
What Models Tell Us About the Evolution of Carbon Sources and Sinks over the Phanerozoic <i>Y. Godd��ris, Y. Donnadieu, and B.J.W. Mills</i>	471
The Rock-Hosted Biosphere <i>Alexis S. Templeton and Tristan A. Caro</i>	493
Petrogenesis and Geodynamic Significance of Xenolithic Eclogites <i>Sonja Aulbach and Katie A. Smart</i>	521
A Systems Approach to Understanding How Plants Transformed Earth's Environment in Deep Time <i>William J. Mattheaeus, Sophia I. Macarewich, Jon Richey, Isabel P. Monta��ez, Jennifer C. McElwain, Joseph D. White, Jonathan P. Wilson, and Christopher J. Poulsen</i>	551
Ductile Deformation of the Lithospheric Mantle <i>Jessica M. Warren and Lars N. Hansen</i>	581
Frontiers of Carbonate Clumped Isotope Thermometry <i>Katharine W. Huntington and Sierra V. Petersen</i>	611
Mars Seismology <i>P. Lognonn��, W.B. Banerdt, J. Clinton, R.F. Garcia, D. Giardini, B. Knappmeyer-Endrun, M. Panning, and W.T. Pike</i>	643
The Role of Giant Impacts in Planet Formation <i>Travis S.J. Gabriel and Saverio Cambioni</i>	671

Errata

An online log of corrections to *Annual Review of Earth and Planetary Sciences* articles may be found at <http://www.annualreviews.org/errata/earth>

Related Articles

From the *Annual Review of Astronomy and Astrophysics*, Volume 60 (2022)

Atmospheres of Rocky Exoplanets

Robin Wordsworth and Laura Kreidberg

From the *Annual Review of Chemical and Biomolecular Engineering*, Volume 13 (2022)

Direct Air Capture of CO₂ Using Solvents

Radu Custelcean

Technological Options for Direct Air Capture: A Comparative Process
Engineering Review

Xiaowei Wu, Ramanan Krishnamoorti, and Praveen Bollini

From the *Annual Review of Ecology, Evolution, and Systematics*, Volume 53 (2022)

Evolutionary Ecology of Fire

Jon E. Keeley and Juli G. Pausas

Integrating Fossil Observations Into Phylogenetics Using the Fossilized
Birth–Death Model

*April M. Wright, David W. Bapst, Joëlle Barido-Sottani,
and Rachel C.M. Warnock*

The Macroevolutionary History of Bony Fishes: A Paleontological View

Matt Friedman

From the *Annual Review of Environment and Resources*, Volume 47 (2022)

The Ocean Carbon Cycle

Tim DeVries

Permafrost and Climate Change: Carbon Cycle Feedbacks From
the Warming Arctic

*Edward A.G. Schuur, Benjamin W. Abbott, Roisin Commane, Jessica Ernakovich,
Eugenie Euskirchen, Gustaf Hugelius, Guido Grosse, Miriam Jones, Charlie Koven,
Victor Leshyk, David Lawrence, Michael M. Loranty, Marguerite Mauritz,
David Olefeldt, Susan Natali, Heidi Rodenhizer, Verity Salmon, Christina Schädel,
Jens Strauss, Claire Treat, and Merritt Turetsky*

Remote Sensing the Ocean Biosphere

Sam Purkis and Ved Chirayath

From the *Annual Review of Fluid Mechanics*, Volume 55 (2023)

Submesoscale Dynamics in the Upper Ocean

John R. Taylor and Andrew F. Thompson

Fluid Dynamics of Polar Vortices on Earth, Mars, and Titan

Darryn W. Waugh

Icebergs Melting

Claudia Cenedese and Fiamma Straneo

The Fluid Mechanics of Deep-Sea Mining

Thomas Peacock and Raphael Ouillon

Turbulent Rotating Rayleigh–Bénard Convection

Robert E. Ecke and Olga Shishkina

From the *Annual Review of Marine Science*, Volume 15 (2023)

From Stamps to Parabolas

S. George Philander

Sociotechnical Considerations About Ocean Carbon Dioxide Removal

Sarah R. Cooley, Sonja Klinsky, David R. Morrow, and Terre Satterfield

Nuclear Reprocessing Tracers Illuminate Flow Features and Connectivity

Between the Arctic and Subpolar North Atlantic Oceans

Núria Casacuberta and John N. Smith

The Arctic Ocean's Beaufort Gyre

Mary-Louise Timmermans and John M. Toole

Global Quaternary Carbonate Burial: Proxy- and Model-Based Reconstructions
and Persisting Uncertainties

Madison Wood, Christopher T. Hayes, and Adina Paytan

Quantifying the Ocean's Biological Pump and Its Carbon Cycle Impacts
on Global Scales

David A. Siegel, Timothy DeVries, Ivona Cetinić, and Kelsey M. Bisson

Novel Insights into Marine Iron Biogeochemistry from Iron Isotopes

Jessica N. Fitzsimmons and Tim M. Conway

Insights from Fossil-Bound Nitrogen Isotopes in Diatoms, Foraminifera,
and Corals

*Rebecca S. Robinson, Sandi M. Smart, Jonathan D. Cybulski, Kelton W. McMahon,
Basia Marcks, and Catherine Nowakowski*

Prokaryotic Life in the Deep Ocean's Water Column

Gerhard J. Herndl, Barbara Bayer, Federico Baltar, and Thomas Reinthaler

Lipid Biogeochemistry and Modern Lipidomic Techniques

Bethanie R. Edwards

From the *Annual Review of Materials Research*, Volume 52 (2022)

Biomaterialized Materials for Sustainable and Durable Construction

Danielle N. Beatty, Sarah L. Williams, and Wil V. Sruhar III

Brittle Solids: From Physics and Chemistry to Materials Applications

Brian R. Lawn and David B. Marshall

Material Flows and Efficiency

Jonathan M. Cullen and Daniel R. Cooper

Architectural Glass

Sheldon M. Wiederborn and David R. Clarke